

Derivation and analysis on the analytical structure of interval type-2 fuzzy controller with two nonlinear fuzzy sets for each input variable*

Bin-bin LEI^{†1}, Xue-chao DUAN¹, Hong BAO¹, Qian XU²

(¹MOE Key Laboratory of Electronic Equipment Structure Design, Xidian University, Xi'an 710071, China)

(²Xinjiang Observatory, National Astronomical Observatories, Chinese Academy of Sciences, Urumqi 830011, China)

[†]E-mail: 18717368076@163.com

Received Feb. 23, 2016; Revision accepted Apr. 28, 2016; Crosschecked May 23, 2016

Abstract: Type-2 fuzzy controllers have been mostly viewed as black-box function generators. Revealing the analytical structure of any type-2 fuzzy controller is important as it will deepen our understanding of how and why a type-2 fuzzy controller functions and lay a foundation for more rigorous system analysis and design. In this study, we derive and analyze the analytical structure of an interval type-2 fuzzy controller that uses the following identical elements: two nonlinear interval type-2 input fuzzy sets for each variable, four interval type-2 singleton output fuzzy sets, a Zadeh AND operator, and the Karnik-Mendel type reducer. Through dividing the input space of the interval type-2 fuzzy controller into 15 partitions, the input-output relationship for each local region is derived. Our derivation shows explicitly that the controller is approximately equivalent to a nonlinear proportional integral or proportional differential controller with variable gains. Furthermore, by comparing with the analytical structure of its type-1 counterpart, potential advantages of the interval type-2 fuzzy controller are analyzed. Finally, the reliability of the analysis results and the effectiveness of the interval type-2 fuzzy controller are verified by a simulation and an experiment.

Key words: Interval type-2 fuzzy controller, Analytical structure, Karnik-Mendel type reducer

<http://dx.doi.org/10.1631/FITEE.1601019>

CLC number: TP13


1 Introduction

Numerical studies have shown that the interval type-2 (IT2) fuzzy controller can outperform its type-1 (T1) counterpart in the faces of complicated imprecision and uncertainty (Du and Ying, 2007; Hagrass, 2007; Mendel, 2007; Zhou *et al.*, 2009; Lin, 2015). Although the advantages of the IT2 fuzzy controllers have been demonstrated through case studies, the controllers are still treated as black boxes

and cannot be amenable for analysis and interpretation by engineers.

Analytical structure means a mathematical expression that precisely describes the input-output relationship of a controller. Once the analytical structure is available, one can have a deeper understanding of the IT2 fuzzy controller and on how it functions, and can also provide guidelines for the system design of the IT2 fuzzy controller. In the past two decades, researchers have investigated the analytical structure of various T1 fuzzy controllers (Ying *et al.*, 1990; Haj-Ali and Ying, 2004; Li and Shen, 2009). Because the IT2 fuzzy controller is more complicated than its T1 counterpart, deriving the analytical structure of the IT2 fuzzy controller is difficult, especially when the IT2 fuzzy controller involves the Zadeh AND operator. The analytical

* Project supported by the Xinjiang Astronomical Observatory, China (No. 2014KL012), the Major State Basic Research Development Program of China (No. 2015CB857100), the National Natural Science Foundation of China (Nos. 51490660 and 51405362), and the Fundamental Research Funds for the Central Universities, China (No. SPSY021401)

 ORCID: Bin-bin LEI, <http://orcid.org/0000-0003-3612-5625>

© Zhejiang University and Springer-Verlag Berlin Heidelberg 2016

derivations of the IT2 fuzzy proportional integral (PI) or proportional differential (PD) controller were obtained by dividing the input space into several partitions (Du and Ying, 2010; Nie and Tan, 2012). An effort was made to derive the analytical structure for a broad class of typical IT2 Mamdani fuzzy controllers which use arbitrary fuzzy rules with any number and types of IT2 fuzzy sets (Zhou and Ying, 2013). An innovative analytical structure derivation technique for TS IT2 fuzzy controllers, whose configurations are two linear IT2 fuzzy sets for each input variable and linear TS fuzzy rules, was proposed in Zhou and Ying (2014). So far, a very limited amount of research has been conducted to address the analytical structure of an IT2 controller, all focusing on the controller which involves linear IT2 fuzzy sets for input variables (Du and Ying, 2010; Nie and Tan, 2012; Zhou and Ying, 2012; 2013; 2014). No research has focused on the analytical structure of the IT2 fuzzy controller involving nonlinear IT2 fuzzy sets.

The contributions of this work are as follows: (1) A method is presented to extend the structure analysis to the IT2 fuzzy controller which uses the following identical elements: two nonlinear IT2 input fuzzy sets for each variable, four IT2 singleton output fuzzy sets, the Zadeh AND operator, and the Karnik-Mendel (KM) type reducer. (2) An analysis of the variable gains of the analytical structure of the IT2 fuzzy controller is shown. Some guidelines are provided to tune the design parameters of the IT2 fuzzy controller based on the structure information. (3) A theoretical comparison between the IT2 fuzzy controller and its corresponding T1 fuzzy controller is presented to analyze the advantages of the IT2 fuzzy controller. (4) The reliability of the analysis results and the effectiveness of the IT2 fuzzy controller are verified by a simulation and an experiment.

2 Configuration of the IT2 fuzzy controller

A fuzzy controller with two inputs and a single output is widely used in practical engineering (Fig. 1). The fuzzy inputs can be defined as

$$E(n) = K_e e(n) = K_e (\text{ref}(n) - y(n)), \quad (1)$$

$$R(n) = K_r r(n) = K_r (e(n) - e(n-1)), \quad (2)$$

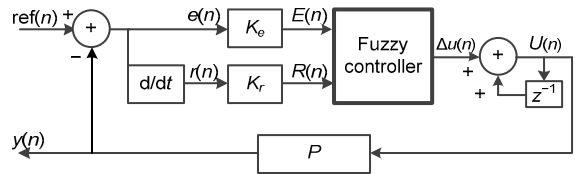


Fig. 1 The structure of the IT2 fuzzy control system

where $E(n)$ is the system error, abbreviated as E , $R(n)$ the rate of the error signal, abbreviated as R , $y(n)$ the controlled variable, $\text{ref}(n)$ the reference signal, and K_e and K_r the scaling factors for $e(n)$ and $r(n)$, respectively. The output of the fuzzy controller denotes the increment of the control input:

$$\Delta u(n) = f(E, R). \quad (3)$$

Fig. 2 shows the IT2 fuzzy sets for the fuzzy inputs. Each input is fuzzified by two IT2 fuzzy sets, namely ‘positive’ (denoted by P) and ‘negative’ (denoted by N). μ_p^1 and μ_N^1 are the membership functions of the fuzzy sets for E , and the IT2 fuzzy sets for R are represented by μ_p^2 and μ_N^2 . The upper membership functions (UMFs) and the lower membership functions (LMFs) of the fuzzy sets on each input satisfy the following equations:

$$\bar{\mu}_p^i(x) + \underline{\mu}_N^i(x) = \underline{\mu}_p^i(x) + \bar{\mu}_N^i(x) = 1, \quad (4)$$

$$\bar{\mu}_p^i(-\theta_i) = \underline{\mu}_N^i(-\theta_i) = \underline{\mu}_p^i(\theta_i) = \bar{\mu}_N^i(\theta_i) = 0.5, \quad (5)$$

where x is the input variable (E or R), $\bar{\mu}^i$ and $\underline{\mu}^i$ ($i=1, 2$) the upper and lower bounds of its primary membership, respectively, and θ_i ($i=1, 2$) the design parameter. For example, the UMFs and LMFs for input E are

$$\left\{ \begin{array}{l} \overline{EP} = \bar{\mu}_p^1(E) = \frac{1}{1 + \exp(-E - \theta_1)}, \\ \underline{EP} = \underline{\mu}_p^1(E) = \frac{1}{1 + \exp(-E + \theta_1)}, \\ \overline{EN} = \bar{\mu}_N^1(E) = \frac{1}{1 + \exp(E - \theta_1)}, \\ \underline{EN} = \underline{\mu}_N^1(E) = \frac{1}{1 + \exp(E + \theta_1)}. \end{array} \right. \quad (6)$$

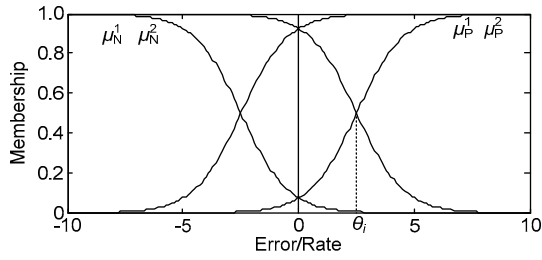


Fig. 2 The IT2 antecedent fuzzy sets of error and rate

The UMFs and LMFs for input R are

$$\left\{ \begin{array}{l} \overline{\text{RP}} = \overline{\mu}_P^2(R) = \frac{1}{1 + \exp(-R - \theta_2)}, \\ \underline{\text{RP}} = \underline{\mu}_P^2(R) = \frac{1}{1 + \exp(-R + \theta_2)}, \\ \overline{\text{RN}} = \overline{\mu}_N^2(R) = \frac{1}{1 + \exp(R - \theta_2)}, \\ \underline{\text{RN}} = \underline{\mu}_N^2(R) = \frac{1}{1 + \exp(R + \theta_2)}. \end{array} \right. \quad (7)$$

As shown in Fig. 2, the UMF and LMF jointly determine the foot print of uncertainty (FOU) of an IT2 fuzzy set. So, we can adjust the size of the FOU by changing parameters θ_1 and θ_2 , which can make an improvement to the system's control performance.

For the fuzzy system whose IT2 fuzzy sets for inputs are shown in Fig. 2, the rule base is listed below:

Rule 1 If $E(n)$ is positive and $R(n)$ is positive, then $\Delta u(n)$ is H_1 .

Rule 2 If $E(n)$ is positive and $R(n)$ is negative, then $\Delta u(n)$ is H_2 .

Rule 3 If $E(n)$ is negative and $R(n)$ is positive, then $\Delta u(n)$ is H_3 .

Rule 4 If $E(n)$ is negative and $R(n)$ is negative, then $\Delta u(n)$ is H_4 .

Here, $H_1, H_2, H_3,$ and H_4 are singleton fuzzy sets.

Based on the Zadeh AND operator, the firing sets of the four rules are as follows:

$$F^1 = [\underline{f}^1, \overline{f}^1] = [\min(\underline{\text{EP}}, \underline{\text{RP}}), \min(\overline{\text{EP}}, \overline{\text{RP}})], \quad (8)$$

$$F^2 = [\underline{f}^2, \overline{f}^2] = [\min(\underline{\text{EP}}, \underline{\text{RN}}), \min(\overline{\text{EP}}, \overline{\text{RN}})], \quad (9)$$

$$F^3 = [\underline{f}^3, \overline{f}^3] = [\min(\underline{\text{EN}}, \underline{\text{RP}}), \min(\overline{\text{EN}}, \overline{\text{RP}})], \quad (10)$$

$$F^4 = [\underline{f}^4, \overline{f}^4] = [\min(\underline{\text{EN}}, \underline{\text{RN}}), \min(\overline{\text{EN}}, \overline{\text{RN}})]. \quad (11)$$

For this study, the IT2 fuzzy controller uses the KM type-reduction method. Hence, the output of the inference engine can be type-reduced into a T1 fuzzy set consisting of the centroids of all embedded T1 fuzzy sets. The type-reduced set may be expressed mathematically as $Y=[y_l, y_r]$. The centroid of an arbitrary embedded T1 fuzzy set is

$$y = \frac{f^1 H_1 + f^2 H_2 + f^3 H_3 + f^4 H_4}{f^1 + f^2 + f^3 + f^4}, \quad (12)$$

where $f^i \in F^i = [\underline{f}^i, \overline{f}^i]$ ($i=1, 2, 3, 4$). Finally, by centroid defuzzification, the crisp output of the IT2 fuzzy controller is

$$\Delta u(n) = \frac{y_l + y_r}{2}. \quad (13)$$

To simplify the derivation of the analytical structure of the IT2 fuzzy controller, we make the following assumptions: (1) the rule consequents are symmetrical, i.e., $H_2=H_3$, and (2) $H_4 < H_2=H_3 < H_1$.

3 Derivation of the analytical structure of the IT2 fuzzy controller

3.1 Partition of the input space

In the previous section, the type-reduced set is obtained first. Since it is assumed that $H_4 < H_2=H_3 < H_1$, the bounds of the type-reduced set can be expressed as

$$y_l = \frac{\sum_{i=1}^{L-1} \underline{f}^i H_i + \sum_{i=L}^4 \overline{f}^i H_i}{\sum_{i=1}^{L-1} \underline{f}^i + \sum_{i=L}^4 \overline{f}^i}, \quad (14)$$

$$y_r = \frac{\sum_{i=1}^{R-1} \overline{f}^i H_i + \sum_{i=R}^4 \underline{f}^i H_i}{\sum_{i=1}^{R-1} \overline{f}^i + \sum_{i=R}^4 \underline{f}^i}, \quad (15)$$

and the switch points L and R satisfy the following inequalities:

$$H_L \leq y_l < H_{L-1}, \quad (16)$$

$$H_R \leq y_r < H_{R-1}. \quad (17)$$

Because the switch points L and R must be

placed at one of the three singleton fuzzy sets, it can be concluded that L and R can have only one of two values: $H_L = \{H_4, H_3=H_2\}$ and $H_R = \{H_4, H_3=H_2\}$. As an example, to calculate the left point of the type-reduced set, the only two possible cases can be written as follows:

Case 1: If $H_4 \leq y_1 \leq H_3=H_2$, i.e., $L=4$, we have

$$y_1 = y_{11} = \frac{\bar{f}^4 H_4 + \underline{f}^3 H_3 + \underline{f}^2 H_2 + \underline{f}^1 H_1}{\bar{f}^4 + \underline{f}^3 + \underline{f}^2 + \underline{f}^1}. \quad (18)$$

Case 2: If $H_3=H_2 \leq y_1 \leq H_1$, i.e., $L=2$, we have

$$y_1 = y_{12} = \frac{\bar{f}^4 H_4 + \bar{f}^3 H_3 + \bar{f}^2 H_2 + \underline{f}^1 H_1}{\bar{f}^4 + \bar{f}^3 + \bar{f}^2 + \underline{f}^1}. \quad (19)$$

By analyzing Eqs. (18) and (19) for cases 1 and 2, respectively, the following properties can be obtained:

1. The weights which are associated with H_1 and H_4 remain constant, no matter which switch points L and R choose.

2. In case 1, the weights of H_2 and H_3 are the lower bounds of the corresponding firing sets. However, the upper bounds of the corresponding firing sets are chosen to weight H_2 and H_3 in case 2. The condition in which the inference engine changes from case 1 to case 2 can be established as

$$y_1 = y_{11} = y_{12} = H_2 = H_3. \quad (20)$$

By substituting y_{11} and y_{12} with their corresponding expressions in Eqs. (18) and (19), Eq. (20) can be rewritten as

$$\begin{aligned} & \frac{\bar{f}^4 H_4 + \underline{f}^3 H_3 + \underline{f}^2 H_2 + \underline{f}^1 H_1}{\bar{f}^4 + \underline{f}^3 + \underline{f}^2 + \underline{f}^1} \\ &= \frac{\bar{f}^4 H_4 + \bar{f}^3 H_3 + \bar{f}^2 H_2 + \underline{f}^1 H_1}{\bar{f}^4 + \bar{f}^3 + \bar{f}^2 + \underline{f}^1} = H_2 = H_3 \quad (21) \\ & \Leftrightarrow \bar{f}^4 (H_4 - H_2) = \underline{f}^1 (H_2 - H_1) \\ & \Leftrightarrow \bar{f}^4 (H_4 - H_3) = \underline{f}^1 (H_3 - H_1). \end{aligned}$$

According to the assumption that the three consequent sets are uniformly distributed and $H_4 < H_2 = H_3 < H_1$, the condition can be simplified to

$$\bar{f}^4 = \underline{f}^1. \quad (22)$$

Furthermore, when case 1 is used to calculate the left point of the type-reduced set, the condition can be established as

$$y_{11} \leq H_2 = H_3 \Leftrightarrow \bar{f}^4 \geq \underline{f}^1, \quad (23)$$

and the condition in which case 2 is chosen is the following inequality:

$$y_{12} \geq H_2 = H_3 \Leftrightarrow \bar{f}^4 \leq \underline{f}^1. \quad (24)$$

Through observing conditions (23) and (24), to derive the analytical structure of the IT2 fuzzy controller, the firing strengths of rules 1 and 4 must be first specified according to the Zadeh AND operator. Furthermore, whether the controller operates in case 1 or 2 can be determined by comparing the firing strengths of rules 1 and 4. Finally, the partitions of the input space can be found by calculating the firing strengths of rules 2 and 3.

In what follows, an algorithm is introduced to divide the input space by the left point y_1 in the case of $\theta_1 > \theta_2$.

1. The input space is partitioned into a number of regions according to the results of the Zadeh AND operator in \underline{f}^1 and \bar{f}^4 .

(1) The firing strength of rule 1 is defined as

$$\underline{f}^1 = \min(\underline{EP}, \underline{RP}).$$

As shown in Fig. 3a, two regions, IC1 and IC2, are obtained on the input space, where the firing strength \underline{f}^1 is \underline{EP} and \underline{RP} , respectively.

(2) The firing strength of rule 4 can be calculated via

$$\bar{f}^4 = \min(\overline{EN}, \overline{RN}).$$

The input space is divided into two regions, IC1 and IC2 (Fig. 3b), where the firing strength \bar{f}^4 is \overline{EN} and \overline{RN} , respectively.

2. According to conditions (23) and (24), \underline{f}^1 and

\bar{f}^4 are compared to partition the input space into two regions: case 1 and case 2 (Fig. 4).

3. The input space is partitioned according to the firing strength of rules 2 and 3.

(1) In region case 1, the firing strengths of rule 2 and rule 3 are defined as

$$\underline{f}^2 = \min(\underline{EP}, \underline{RN}),$$

$$\underline{f}^3 = \min(\underline{EN}, \underline{RP}).$$

The results of partitioning the region case 1 are shown as the dashed lines in Figs. 5a and 5b, respectively.

(2) In region case 2, the firing strengths of rules 2 and 3 can be calculated via

$$\bar{f}^2 = \min(\bar{EP}, \bar{RN}),$$

$$\bar{f}^3 = \min(\bar{EN}, \bar{RP}).$$

As shown in Fig. 5, these two Zadeh AND operations do not lead to any further region.

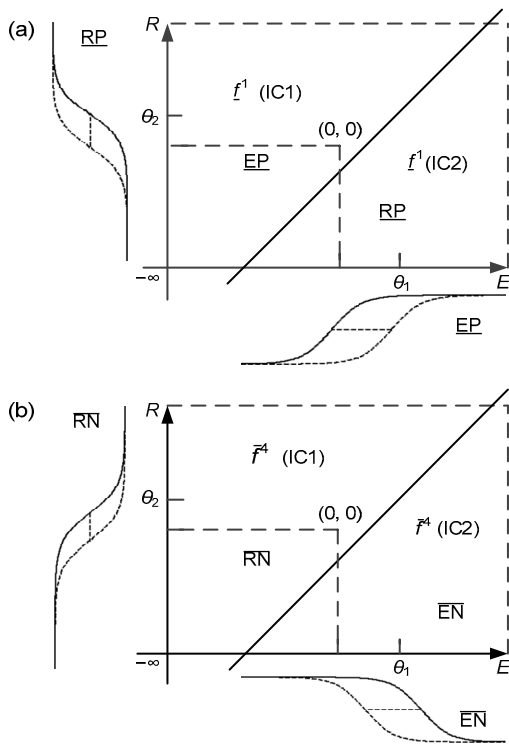


Fig. 3 Partitions by rules 1 and 4: (a) regions divided by \underline{f}^1 ; (b) regions divided by \bar{f}^4

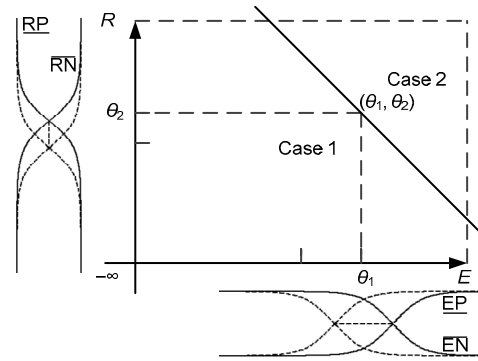


Fig. 4 Boundary that divides the input space into two operating cases in y_1

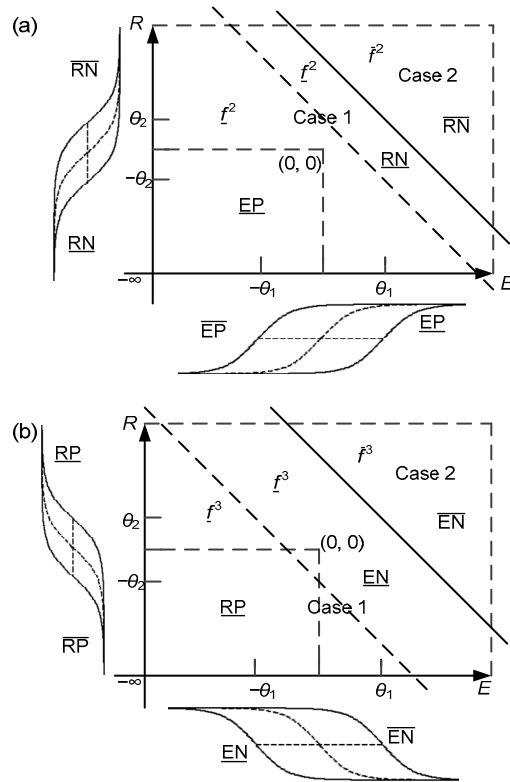


Fig. 5 Partitions by rules 2 and 3: (a) regions by divided by \underline{f}^2 and \bar{f}^2 ; (b) regions divided by \underline{f}^3 and \bar{f}^3

4. Finally, the partition result of the input space by the left point y_l is obtained by superimposing all the results (Fig. 6a). Similarly, by following the proposed algorithm, the partition result of the input space by the right point can be derived (Fig. 6b). Since the output of the IT2 fuzzy controller is the average of the left and right points, the partition result of the input space can be found by superimposing the partition results by y_l and y_r (Fig. 7). The corresponding firing strengths in all local regions are listed in Table 1.

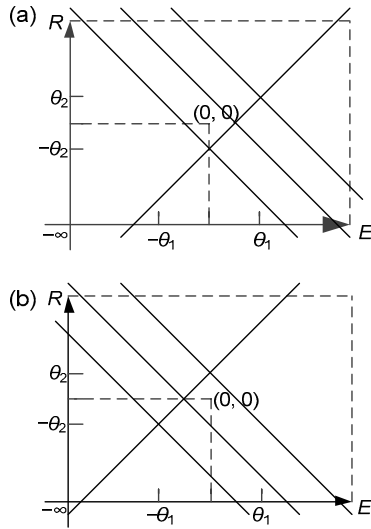


Fig. 6 Partitions of the input space by the left endpoint y_1 (a) and right endpoint y_r (b)

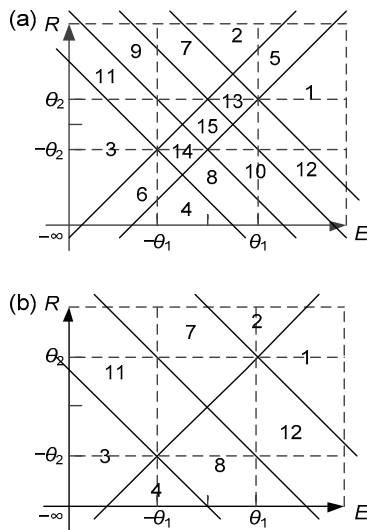


Fig. 7 Partitions of the input space when $\theta_1 \neq \theta_2$ (a) and $\theta_1 = \theta_2$ (b)

3.2 Derivation of input-output expression on each partition of the IT2 fuzzy controller

In this section, mathematical expressions for two points y_1 and y_r on local region IC1 are derived by replacing each firing strength with the corresponding elements in Table 1. The derivation of y_1 and y_r on IC1 is shown as follows:

By replacing the firing strength in Eq. (14) with the corresponding expressions in Table 1, the aforementioned equation can be rewritten as

Table 1 Firing strengths of four rules at y_1 and y_r .

| Region | Rule 1 | | Rule 2 | | Rule 3 | | Rule 4 | |
|--------|------------------|-----------------|------------------|------------------|------------------|------------------|-----------------|------------------|
| | y_1 | y_r | y_1 | y_r | y_1 | y_r | y_1 | y_r |
| 1 | \underline{RP} | \overline{RP} | \overline{RN} | \underline{RN} | \overline{EN} | \underline{EN} | \overline{EN} | \underline{EN} |
| 2 | \underline{EP} | \overline{EP} | \overline{RN} | \underline{RN} | \overline{EN} | \underline{EN} | \overline{RN} | \underline{RN} |
| 3 | \underline{EP} | \overline{EP} | \underline{EP} | \overline{EP} | \underline{RP} | \overline{RP} | \overline{RN} | \underline{RN} |
| 4 | \underline{RP} | \overline{RP} | \underline{EP} | \overline{EP} | \underline{RP} | \overline{RP} | \overline{EN} | \underline{EN} |
| 5 | \underline{EP} | \overline{RP} | \overline{RN} | \underline{RN} | \overline{EN} | \underline{EN} | \overline{RN} | \underline{EN} |
| 6 | \underline{EP} | \overline{RP} | \underline{EP} | \overline{EP} | \underline{RP} | \overline{RP} | \overline{RN} | \underline{EN} |
| 7 | \underline{EP} | \overline{EP} | \overline{RN} | \underline{RN} | \overline{EN} | \underline{EN} | \overline{RN} | \underline{RN} |
| 8 | \underline{RP} | \overline{RP} | \underline{EP} | \overline{EP} | \underline{RP} | \overline{RP} | \overline{EN} | \underline{EN} |
| 9 | \underline{EP} | \overline{EP} | \underline{EP} | \overline{EP} | \overline{EN} | \underline{EN} | \overline{RN} | \underline{RN} |
| 10 | \underline{RP} | \overline{RP} | \underline{EP} | \overline{EP} | \overline{EN} | \underline{EN} | \overline{EN} | \underline{EN} |
| 11 | \underline{EP} | \overline{EP} | \underline{EP} | \overline{EP} | \underline{RP} | \overline{RP} | \overline{RN} | \underline{RN} |
| 12 | \underline{RP} | \overline{RP} | \overline{RN} | \underline{RN} | \overline{EN} | \underline{EN} | \overline{EN} | \underline{EN} |
| 13 | \underline{EP} | \overline{RP} | \overline{RN} | \underline{RN} | \overline{EN} | \underline{EN} | \overline{RN} | \underline{EN} |
| 14 | \underline{EP} | \overline{RP} | \underline{EP} | \overline{EP} | \underline{RP} | \overline{RP} | \overline{RN} | \underline{EN} |
| 15 | \underline{EP} | \overline{RP} | \underline{EP} | \overline{EP} | \overline{EN} | \underline{EN} | \overline{RN} | \underline{EN} |

$$\begin{aligned}
 y_1 &= \frac{\underline{RP} \cdot H_1 + \overline{RN} \cdot H_2 + \overline{EN} \cdot H_3 + \overline{EN} \cdot H_4}{\underline{RP} + \overline{RN} + \overline{EN} + \overline{EN}} \\
 &= \frac{(\underline{RP} - \overline{EN})H}{2\overline{EN} + 1} \\
 &= \frac{1}{1 + \exp(-(R - \theta_2))} \frac{1}{1 + \exp(E - \theta_1)} H \quad (25) \\
 &= \frac{1}{\frac{2}{1 + \exp(E - \theta_1)} + 1} H \\
 &= \frac{\exp(E + R)\exp(-\theta_1 - \theta_2) - 1}{(3 + \exp(E - \theta_1))(1 + \exp(R - \theta_2))} H.
 \end{aligned}$$

Since the Taylor series of $\exp(E+R)$ is

$$\begin{aligned}
 \exp(E+R) &= 1 + (E+R) + \frac{(E+R)^2}{2!} + \frac{(E+R)^3}{3!} + \dots \\
 &= 1 + (E+R) \left(1 + \frac{E+R}{2!} + \frac{(E+R)^2}{3!} + \dots \right), \quad (26)
 \end{aligned}$$

to simplify the derivation of the output expression of the IT2 fuzzy controller, we can make the following assumptions:

$$P_1 = \exp(\theta_1), P_2 = \exp(-\theta_1), P_3 = \exp(\theta_2), P_4 = \exp(-\theta_2), \quad (27)$$

$$\beta_1(E, R) = 1 + \frac{E + R}{2!} + \frac{(E + R)^2}{3!} + \dots \quad (28)$$

Substituting Eqs. (27) and (28) into Eq. (25), the simplified expression of y_l is obtained:

$$\begin{aligned} y_l &= \frac{(P_2 P_4 \beta_1(E, R)(E + R) + P_2 P_4 - 1)H}{(3 + \exp(E - \theta_1))(1 + \exp(R - \theta_2))} \\ &= \frac{P_2 P_4 H \beta_1(E, R)}{(3 + \exp(E - \theta_1))(1 + \exp(R - \theta_2))} R \\ &\quad + \frac{P_2 P_4 H \beta_1(E, R)}{(3 + \exp(E - \theta_1))(1 + \exp(R - \theta_2))} E \\ &\quad + \frac{(P_2 P_4 - 1)H}{(3 + \exp(E - \theta_1))(1 + \exp(R - \theta_2))}. \end{aligned} \quad (29)$$

Similarly, the right point y_r of IC1 is derived as the following expression:

$$\begin{aligned} y_r &= \frac{P_1 P_3 H \beta_1(E, R)}{(3 + \exp(E + \theta_1))(1 + \exp(R + \theta_2))} R \\ &\quad + \frac{P_1 P_3 H \beta_1(E, R)}{(3 + \exp(E + \theta_1))(1 + \exp(R + \theta_2))} E \\ &\quad + \frac{(P_1 P_3 - 1)H}{(3 + \exp(E + \theta_1))(1 + \exp(R + \theta_2))}. \end{aligned} \quad (30)$$

Then, the crisp output expression of the IT2 fuzzy controller in the incremental form is given by

$$\begin{aligned} \Delta u_{IC_1} &= \frac{y_l + y_r}{2} \\ &= \left[\frac{P_2 P_4 H \beta_1(E, R)}{2(3 + \exp(E - \theta_1))(1 + \exp(R - \theta_2))} \right. \\ &\quad \left. + \frac{P_1 P_3 H \beta_1(E, R)}{2(3 + \exp(E + \theta_1))(1 + \exp(R + \theta_2))} \right] R \\ &\quad + \left[\frac{P_2 P_4 H \beta_1(E, R)}{2(3 + \exp(E - \theta_1))(1 + \exp(R - \theta_2))} \right. \\ &\quad \left. + \frac{P_1 P_3 H \beta_1(E, R)}{2(3 + \exp(E + \theta_1))(1 + \exp(R + \theta_2))} \right] E \\ &\quad + \left[\frac{P_2 P_4 - 1}{(3 + \exp(E - \theta_1))(1 + \exp(R - \theta_2))} \right. \\ &\quad \left. + \frac{P_1 P_3 - 1}{(3 + \exp(E + \theta_1))(1 + \exp(R + \theta_2))} \right] H \\ &= K_p^1 R + K_i^1 E + \delta^1. \end{aligned} \quad (31)$$

In other local regions, the derivations of the output of the IT2 fuzzy controller are similar to the process described above for IC1. The expressions on each local region are listed in the Appendix (Eqs. (A8)–(A21)).

In the light of observing the output expressions of the IT2 fuzzy controller, the relationship between the output and inputs on each local region can be written in the following form:

$$\Delta u_{IC_q} = K_p^q R + K_i^q E + \delta^q, \quad (32)$$

where Δu_{IC_q} is the output of the fuzzy controller on local region IC_q , K_p^q the corresponding proportional gain, K_i^q the integral gain, and δ^q the offset.

Through the above work, the IT2 fuzzy controller is proved to be approximately equivalent to a nonlinear PI controller with variable gains. It can also be approximately equivalent to a nonlinear PD controller with variable gains, when the control signal is directly defined as the output of the fuzzy controller.

4 Analysis of the analytical structure of the IT2 fuzzy controller

Fig. 7a shows that the input space of the IT2 fuzzy controller is divided into 15 partitions. To reveal the potential advantages of the IT2 fuzzy controller, this section focuses on analyzing the expressions of the control signals on every local region derived in the above section and comparing with its T1 counterpart.

The membership functions of the antecedent sets for the T1 fuzzy controller are as follows (Fig. 8):

$$\begin{cases} \mu_p(E) = \frac{1}{1 + e^{-E}}, \\ \mu_n(E) = \frac{1}{1 + e^E}, \end{cases} \quad (33)$$

$$\begin{cases} \eta_p(R) = \frac{1}{1 + e^{-R}}, \\ \eta_n(R) = \frac{1}{1 + e^R}. \end{cases} \quad (34)$$

Fig. 9 shows the partition of the input space of the T1 controller using the method introduced in the previous section. Under assumption (28), the output of the T1 fuzzy controller on each local region is derived as follows:

1. IC1

$$\Delta u_{IC_1} = \frac{\beta_1 H}{(3 + e^E)(1 + e^R)} E + \frac{\beta_1 H}{(3 + e^E)(1 + e^R)} R, \quad (35)$$

2. IC2

$$\Delta u_{IC_2} = \frac{\beta_1 H}{(1 + e^E)(3 + e^R)} E + \frac{\beta_1 H}{(1 + e^E)(3 + e^R)} R, \quad (36)$$

3. IC3

$$\Delta u_{IC_3} = \frac{\beta_1 H}{(1 + 3e^E)(1 + e^R)} E + \frac{\beta_1 H}{(1 + 3e^E)(1 + e^R)} R, \quad (37)$$

4. IC4

$$\Delta u_{IC_4} = \frac{\beta_1 H}{(1 + e^E)(1 + 3e^R)} E + \frac{\beta_1 H}{(1 + e^E)(1 + 3e^R)} R. \quad (38)$$

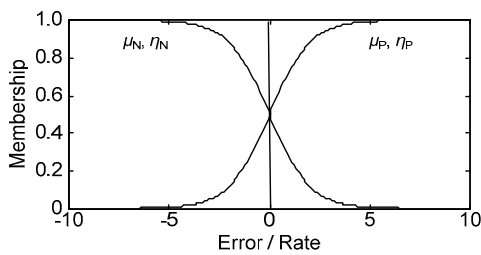


Fig. 8 T1 antecedent fuzzy sets

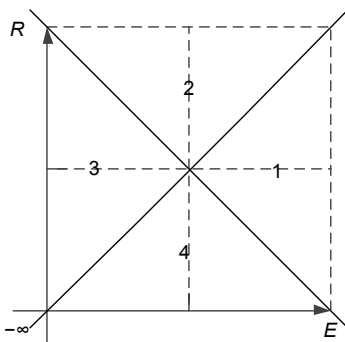


Fig. 9 Partition of the input space of the T1 controller

4.1 Relationship between design parameters and regions

Figs. 7a and 7b show the partitions of the input space for $\theta_1 \neq \theta_2$ and $\theta_1 = \theta_2$, respectively. By comparing these two figures, some regions exist only when $\theta_1 \neq \theta_2$, such as IC5 and IC6, IC9 and IC10, and IC13–IC15. It is obvious that the sizes of these regions are determined by $|\theta_1 - \theta_2|$. The smaller the difference between θ_1 and θ_2 , the smaller the sizes of these regions.

The derived expressions of the regions which exist under condition $\theta_1 \neq \theta_2$ (IC5–IC6, IC9–IC10, and IC13–IC15, see the Appendix) indicate that the type-reduced sets of these regions are related to that of its adjacent regions. For example, as shown in Fig. 7a, the adjacent regions of IC5 are IC2 and IC1. Then the left point expression of the type-reduced set on IC5 is the same as the counterpart on IC2, and the right point expression is equal to the counterpart on IC1. In other words, these relationships can make the output signal of the IT2 fuzzy controller smoother when the fuzzy controller works from one region to another region which exists only when $\theta_1 \neq \theta_2$.

4.2 Analysis of the derived gains of the IT2 fuzzy controller

In this section, for an easier and more insightful analysis, we focus on the variable gains of the IT2 fuzzy controller on IC1 and IC12 in the case of $\theta_1 = \theta_2$. This analysis method can also be applicable to the IT2 fuzzy controller with unequal design parameters. The main reason why the IC1 and IC12 are selected is that these two regions contain the main control process and the desired point. Eqs. (A8)–(A21) in the Appendix show that the analytical structure of the IT2 fuzzy controller with nonlinear IT2 fuzzy sets is very complex. So, it is difficult to analyze the variable gains of the IT2 fuzzy controller using analytical methods (Nie and Tan, 2012). In this section, we analyze the variable proportional gain on IC1 and IC12 with the help of numerical simulation in MATLAB. The functional relationship between the proportional gain and the fuzzy inputs on IC1 and IC12 is shown in Fig. 10. The design parameters are $\theta_1 = \theta_2 = 0.3$ (Fig. 10a) and $\theta_1 = \theta_2 = 1.0$ (Fig. 10b), respectively.

Fig. 10 shows that the proportional gain is a non-monotonic function with respect to the fuzzy inputs on IC1 and IC12. In addition, we can find that the maximal proportional gain on IC1 increases with

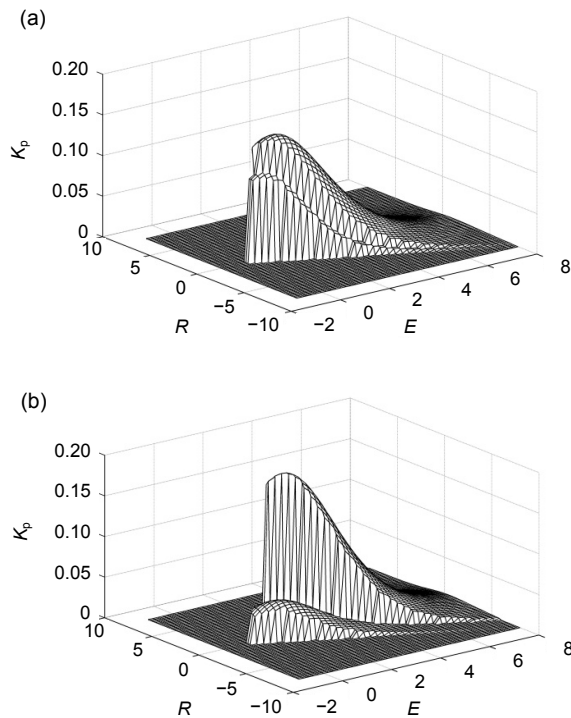


Fig. 10 Proportional gain of the IT2 fuzzy controller on IC1 and IC12: (a) $\theta_1=\theta_2=0.3$; (b) $\theta_1=\theta_2=1.0$

the increase of the design parameters. In contrast, the maximal proportional gain on IC12 decreases when the design parameters increase. Based on these results, if we want to shorten the rising time and reduce the overshoot, the design parameters can be increased appropriately. Therefore, to some extent the analytical structure of the IT2 fuzzy controller can provide a guideline for the design of the IT2 fuzzy controller.

4.3 Comparison between the outputs of the IT2 fuzzy controller and its T1 counterpart

For any given fuzzy input in every local region, the relationship between the output of the IT2 fuzzy controller and that of its T1 counterpart is the focus of this section. Fig. 8 shows the fuzzy sets for the inputs of the T1 controller. Fig. 9 shows the partition results of the input space of the T1 controller. An inspection of Figs. 7 and 9 shows that the local regions of the IT2 controller can be regarded as the subset of the local regions of the T1 counterpart when $\theta_1=\theta_2$. For example, IC1 and IC8 in Fig. 7b can be considered as the subsets of IC1 in Fig. 9. With the load expressions on the regions of the IT2 controller and its T1 counterpart, comparison directly by the analytical method is

difficult. So, the comparative results between the outputs of the IT2 fuzzy controller and its T1 counterpart are obtained by numerical study in MATLAB. Fig. 11 shows the comparison results when $\theta_1=\theta_2$. The ‘plus’ area represents that the output of the T1 controller is larger, and the ‘circle’ area means that the larger one is the output of the IT2 controller.

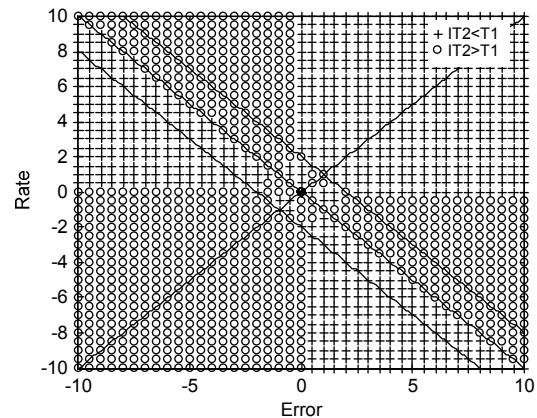


Fig. 11 Comparison between the T1 and IT2 controllers when $\theta_1=\theta_2$

As shown in Fig. 11, for the special case $\theta_1=\theta_2$, when the error is large and the rate of error change is negative, the IT2 fuzzy controller will produce a larger output than its T1 counterpart. This larger control signal may lead to a smaller rising time. When the positive error becomes little, a smaller output of the IT2 controller will attempt to avoid overshooting. Once an overshoot appears and rises, it will be prevented by the larger control signal of the IT2 controller.

Through comparing and analyzing the analytical structures of the IT2 fuzzy controller and its T1 counterpart, we can obtain theoretical analysis conclusions as follows:

1. According to the analytical structure of the proposed IT2 fuzzy controller, increasing the design parameters appropriately helps improve the control performance.
2. Compared with the T1 fuzzy controller, the IT2 fuzzy PI controller can reduce the overshoot and decrease the rising time at the same time.
3. In terms of disturbance rejection, the IT2 fuzzy controller has a stronger robustness than its T1 counterpart.

5 Simulation and experiment

5.1 Simulation

In this study, a coupled-tank is used to demonstrate the proposed IT2 fuzzy controller, whose differential equations are as follows (Wu and Tan, 2007):

$$A_1 \frac{dH_1}{dt} = Q_1 - \alpha_1 \sqrt{H_1} - \alpha_3 \sqrt{H_1 - H_2}, \quad (39)$$

$$A_2 \frac{dH_2}{dt} = Q_2 - \alpha_2 \sqrt{H_2} - \alpha_3 \sqrt{H_1 - H_2}, \quad (40)$$

where A_1 and A_2 are the sectional areas of tanks 1 and 2, respectively, $A_1=A_2=36.52 \text{ cm}^2$, H_1 and H_2 the water levels of tanks 1 and 2, respectively, Q_1 and Q_2 the rates at which water is pumped into tanks 1 and 2, respectively, and α_1 , α_2 , and α_3 are proportionality constants.

The objective is to control the water level H_2 in tank 2 by regulating the amount of water Q_1 . The target level is 15 cm and the following parameters are assumed as $H_1=H_2=0$, $\alpha_1=\alpha_2=5.6186$, $\alpha_3=10$, $Q_2=0$. In this simulation, three fuzzy controllers are used for the coupled-tank system, i.e., No. 1 IT2 fuzzy controller with $\theta_1=1.2$ and $\theta_2=0.12$, No. 2 IT2 fuzzy controller with $\theta_1=0.8$ and $\theta_2=0.12$, and the T1 fuzzy controller mentioned in Section 4. The simulation results are shown in Fig. 12, and the control indexes are summarized in Table 2. The performance index, integral of time multiplied absolute value of error (ITAE), is defined as

$$\text{ITAE} = \int_0^T t |e(t)| dt, \quad (41)$$

where T is the simulation time.

Fig. 12a and Table 2 show that, compared with the T1 fuzzy controller, the IT2 fuzzy controllers significantly reduce the overshoot and setting time, without increasing the rising time. Fig. 12b shows the error versus rate trajectory. We can see that the appropriate increase of the design parameter θ_1 contributes to the overshoot suppression. In terms of overshoot, rising time, and setting time, the simulation results of these three fuzzy controllers are identical to the theoretical analysis in the previous section.

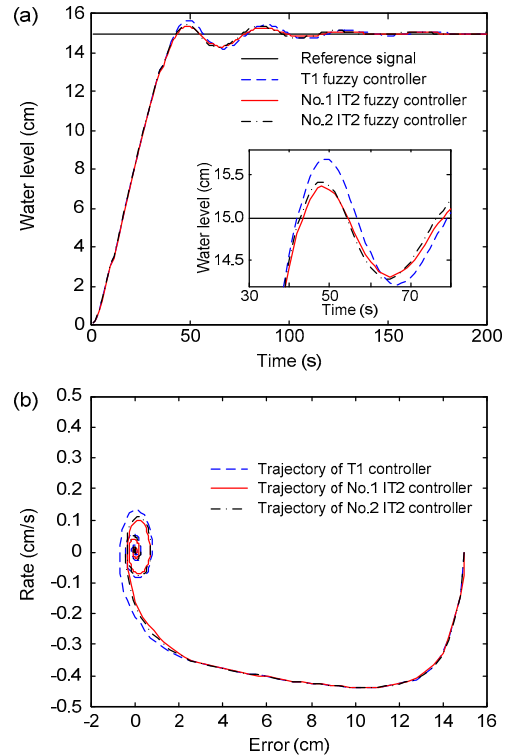


Fig. 12 Results of the coupled-tank water level control simulation: (a) step response of the fuzzy controllers; (b) trajectories of error and rate

Table 2 Comparison of the properties of the step response for the T1 and IT2 fuzzy systems

| Controller | Rising time (s) | Overshoot (%) | Setting time (s) | ITAE |
|------------|-----------------|---------------|------------------|--------|
| T1 | 30 | 4.6289 | 93 | 6747.6 |
| No. 1 IT2 | 30 | 2.4333 | 73 | 5927.9 |
| No. 2 IT2 | 30 | 2.8329 | 88 | 6099.3 |

ITAE: integral of time multiplied absolute value of error

5.2 Experiment

The industrial mechatronics drives unit (IMDU) is an ideal test apparatus for a basic servo system, a reverse compensation, the friction compensation, and an industrial system of high-order system coupling (Fig. 13). The IMDU is equipped with four axes of rotation, among which two are motor drivers and the others are free rotations. All four axes are equipped with an optical encoder. The motor is controlled by a 100-W linear amplifier.

The experiment is the angular position sinusoidal tracking on a drive shaft under the load condition, where uniform white noise is added to the system output. The performances of the IT2 fuzzy controller

and its T1 counterpart are compared by the criterion defined as the integral of absolute error (IAE) of the sinusoidal tracking curve. Specific parameter selections are as follows: $K_e=200$, $K_r=0.5$, $H=25$, $\theta_1=0.25$, and $\theta_2=0.4$. The results of the experiment are shown in Fig. 14.



Fig. 13 Industrial mechatronics drives unit

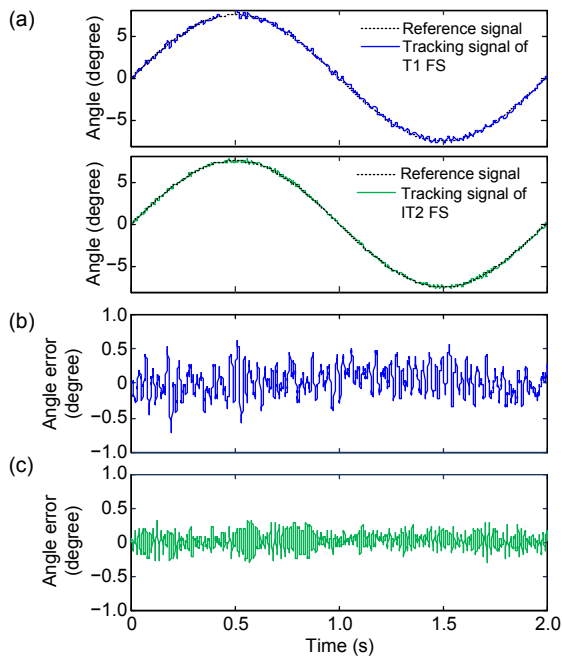


Fig. 14 Results of the sinusoidal tracking experiment: (a) sinusoidal tracking curve of the IT2 fuzzy system and its T1 counterpart; (b) sinusoidal tracking error of the IT2 fuzzy system; (c) sinusoidal tracking error of the T1 fuzzy system

One inference is that the IAE of the T1 controller is 3381.4 in a sinusoidal cycle. However, the IAE of the IT2 fuzzy controller amounts only to 1769.3, and the control performance is improved by 47.7%. The results of this experiment imply that the IT2 fuzzy controller can outperform its T1 counterpart in terms of tackling system disturbance. This means that the IT2 fuzzy controller has a stronger robustness.

6 Conclusions

The analytical structure deriving method for the IT2 fuzzy controller with nonlinear fuzzy sets is shown in this paper. The main contributions of this work can be drawn as follows:

1. The analytical structure derivation of the IT2 fuzzy controller is extended to the IT2 fuzzy controller with nonlinear IT2 fuzzy sets and the Zadeh AND operator.

2. Through dividing the input space of the IT2 fuzzy controller into 15 partitions, the controller is demonstrated to be approximately equivalent to a nonlinear PI or PD controller with variable gains.

3. The analytical structure deepens the understanding of the internal input-output relationships of the IT2 fuzzy controller. A comparative analysis of the derived analytical structure and its T1 counterpart revealed the potential advantages of the IT2 fuzzy controller.

For future work, we are going to provide more guidelines for the system design and stability analysis of the IT2 fuzzy controller by using the analytical structure of the IT2 fuzzy controller.

References

- Du, X.Y., Ying, H., 2007. Control performance comparison between a type-2 fuzzy controller and a comparable conventional Mamdani fuzzy controller. Annual Meeting of the North American Fuzzy Information Processing Society, p.100-105.
<http://dx.doi.org/10.1109/NAFIPS.2007.383819>
- Du, X.Y., Ying, H., 2010. Derivation and analysis of the analytical structures of the interval type-2 fuzzy-PI and PD controllers. *IEEE Trans. Fuzzy Syst.*, **18**(4):802-814.
<http://dx.doi.org/10.1109/TFUZZ.2010.2049022>
- Hagras, H., 2007. Type-2 FLCs: a new generation of fuzzy controllers. *IEEE Comput. Intell. Mag.*, **2**(1):30-43.
<http://dx.doi.org/10.1109/MCI.2007.357192>
- Haj-Ali, A., Ying, H., 2004. Structural analysis of fuzzy controllers with nonlinear input fuzzy sets in relation to nonlinear PID control with variable gains. *Automatica*, **40**(9):1551-1559.
<http://dx.doi.org/10.1016/j.automatica.2004.03.019>
- Li, Q.C., Shen, D.Y., 2009. Brand-new PID fuzzy controller (fuzzy PI+fuzzy PD). *Contr. Dec.*, **24**(7):1037-1042 (in Chinese).
<http://dx.doi.org/10.13195/j.cd.2009.07.80.liqch.015>
- Lin, F.J., 2015. Type-2 fuzzy logic control. *IEEE Syst. Man Cybern. Mag.*, **1**(1):47-48.
<http://dx.doi.org/10.1109/MSMC.2015.2395651>

- Mendel, J.M., 2007. Type-2 fuzzy sets and systems: an overview. *IEEE Comput. Intell. Mag.*, **2**(1):20-29. <http://dx.doi.org/10.1109/MCI.2007.380672>
- Nie, M.W., Tan, W.W., 2012. Analytical structure and characteristics of symmetric Karnik-Mendel type-reduced interval type-2 fuzzy PI and PD controllers. *IEEE Trans. Fuzzy Syst.*, **20**(3):416-430. <http://dx.doi.org/10.1109/TFUZZ.2011.2174061>
- Wu, D.R., Tan, W.W., 2007. A simplified type-2 fuzzy controller for real-time control. *ISA Trans.*, **45**(4):503-516. [http://dx.doi.org/10.1016/S0019-0578\(07\)60228-6](http://dx.doi.org/10.1016/S0019-0578(07)60228-6)
- Ying, H., Siler, W., Buckley, J.J., 1990. Fuzzy control theory: a nonlinear case. *Automatica*, **26**(3):513-520. [http://dx.doi.org/10.1016/0005-1098\(90\)90022-A](http://dx.doi.org/10.1016/0005-1098(90)90022-A)
- Zhou, H.B., Ying, H., 2012. A technique for deriving analytical structure of a general class of interval type-2 TS fuzzy controllers. Annual Meeting of the North American Fuzzy Information Processing Society, p.1-6. <http://dx.doi.org/10.1109/NAFIPS.2012.6290968>
- Zhou, H.B., Ying, H., 2013. A method for deriving the analytical structure of a broad class of typical interval type-2 Mamdani fuzzy controllers. *IEEE Trans. Fuzzy Syst.*, **21**(3):447-458. <http://dx.doi.org/10.1109/TFUZZ.2012.2226891>
- Zhou, H.B., Ying, H., 2014. A method for deriving the analytical structure of the TS fuzzy controllers with two linear interval type-2 fuzzy sets for each input variable. IEEE Int. Conf. on Fuzzy Systems, p.612-618. <http://dx.doi.org/10.1109/fuzz-ieee.2014.6891540>
- Zhou, H.B., Ying, H., Duan, J.A., 2009. Adaptive control using interval type-2 fuzzy logic. IEEE Int. Conf. on Fuzzy Systems, p.836-841. <http://dx.doi.org/10.1109/FUZZY.2009.5277302>

Appendix: Expressions of output of the IT2 fuzzy controller on local regions IC2–IC15

On local regions IC2–IC15, the derivations of the output expression of the IT2 fuzzy controller are similar to the process for IC1 described in Section 3.2. First of all, some assumptions are made in the following:

$$P_1=\exp(\theta_1), P_2=\exp(-\theta_1), P_3=\exp(\theta_2), P_4=\exp(-\theta_2), \quad (\text{A1})$$

$$\beta_1(E, R) = 1 + \frac{E + R}{2!} + \frac{(E + R)^2}{3!} + \dots, \quad (\text{A2})$$

$$\beta_2(E) = 1 + \frac{E}{2!} + \frac{E^2}{3!} + \dots, \quad (\text{A3})$$

$$\beta_3(R) = 1 + \frac{R}{2!} + \frac{R^2}{3!} + \dots, \quad (\text{A4})$$

$$\beta_4(E, R) = 1 + \frac{E + 2R}{2!} + \frac{(E + 2R)^2}{3!} + \dots, \quad (\text{A5})$$

$$\beta_5(E, R) = 1 + \frac{2E + R}{2!} + \frac{(2E + R)^2}{3!} + \dots, \quad (\text{A6})$$

$$\beta_6(E, R) = 1 + \frac{2E + 2R}{2!} + \frac{(2E + 2R)^2}{3!} + \dots. \quad (\text{A7})$$

Then, the expressions of the output of the IT2 fuzzy controller on each local region except IC1 are listed as follows:

1. IC2

$$\Delta u_{IC_2} = \left[\frac{P_2 P_4 H \beta_1(E, R)}{2(1+e^{E-\theta_1})(3+e^{R-\theta_2})} + \frac{P_1 P_3 H \beta_1(E, R)}{2(1+e^{E+\theta_1})(3+e^{R+\theta_2})} \right] R + \left[\frac{P_2 P_4 H \beta_1(E, R)}{2(1+e^{E-\theta_1})(3+e^{R-\theta_2})} + \frac{P_1 P_3 H \beta_1(E, R)}{2(1+e^{E+\theta_1})(3+e^{R+\theta_2})} \right] E \quad (\text{A8})$$

$$+ \left[\frac{(P_2 P_4 - 1)H}{2(1+e^{E-\theta_1})(3+e^{R-\theta_2})} + \frac{(P_1 P_3 - 1)H}{2(1+e^{E+\theta_1})(3+e^{R+\theta_2})} \right].$$

2. IC3

$$\Delta u_{IC_3} = \left[\frac{P_2 P_4 H \beta_1(E, R)}{2(1+3e^{E-\theta_1})(1+e^{R-\theta_2})} + \frac{P_1 P_3 H \beta_1(E, R)}{2(1+3e^{E+\theta_1})(1+e^{R+\theta_2})} \right] R + \left[\frac{P_2 P_4 H \beta_1(E, R)}{2(1+3e^{E-\theta_1})(1+e^{R-\theta_2})} + \frac{P_1 P_3 H \beta_1(E, R)}{2(1+3e^{E+\theta_1})(1+e^{R+\theta_2})} \right] E + \left[\frac{(P_2 P_4 - 1)H}{2(1+3e^{E-\theta_1})(1+e^{R-\theta_2})} + \frac{(P_1 P_3 - 1)H}{2(1+3e^{E+\theta_1})(1+e^{R+\theta_2})} \right]. \tag{A9}$$

3. IC4

$$\Delta u_{IC_4} = \left[\frac{P_2 P_4 H \beta_1(E, R)}{2(1+e^{E-\theta_1})(1+3e^{R-\theta_2})} + \frac{P_1 P_3 H \beta_1(E, R)}{2(1+e^{E+\theta_1})(1+3e^{R+\theta_2})} \right] R + \left[\frac{P_2 P_4 H \beta_1(E, R)}{2(1+e^{E-\theta_1})(1+3e^{R-\theta_2})} + \frac{P_1 P_3 H \beta_1(E, R)}{2(1+e^{E+\theta_1})(1+3e^{R+\theta_2})} \right] E + \left[\frac{(P_2 P_4 - 1)H}{2(1+e^{E-\theta_1})(1+3e^{R-\theta_2})} + \frac{(P_1 P_3 - 1)H}{2(1+e^{E+\theta_1})(1+3e^{R+\theta_2})} \right]. \tag{A10}$$

4. IC5

$$\Delta u_{IC_5} = \left[\frac{P_2 P_4 H \beta_1(E, R)}{2(1+e^{E-\theta_1})(3+e^{R-\theta_2})} + \frac{P_1 P_3 H \beta_1(E, R)}{2(3+e^{E+\theta_1})(1+e^{R+\theta_2})} \right] R + \left[\frac{P_2 P_4 H \beta_1(E, R)}{2(1+e^{E-\theta_1})(3+e^{R-\theta_2})} + \frac{P_1 P_3 H \beta_1(E, R)}{2(3+e^{E+\theta_1})(1+e^{R+\theta_2})} \right] E + \left[\frac{(P_2 P_4 - 1)H}{2(1+e^{E-\theta_1})(3+e^{R-\theta_2})} + \frac{(P_1 P_3 - 1)H}{2(3+e^{E+\theta_1})(1+e^{R+\theta_2})} \right]. \tag{A11}$$

5. IC6

$$\Delta u_{IC_6} = \left[\frac{P_2 P_4 H \beta_1(E, R)}{2(1+3e^{E-\theta_1})(1+e^{R-\theta_2})} + \frac{P_1 P_3 H \beta_1(E, R)}{2(1+e^{E+\theta_1})(1+3e^{R+\theta_2})} \right] R + \left[\frac{P_2 P_4 H \beta_1(E, R)}{2(1+3e^{E-\theta_1})(1+e^{R-\theta_2})} + \frac{P_1 P_3 H \beta_1(E, R)}{2(1+e^{E+\theta_1})(1+3e^{R+\theta_2})} \right] E + \left[\frac{(P_2 P_4 - 1)H}{2(1+3e^{E-\theta_1})(1+e^{R-\theta_2})} + \frac{(P_1 P_3 - 1)H}{2(1+e^{E+\theta_1})(1+3e^{R+\theta_2})} \right]. \tag{A12}$$

6. IC7

$$\Delta u_{IC_7} = \left[\frac{(P_2 P_4 - P_1 P_3) \beta_1(E, R) + 2P_2 \beta_4(E, R) + P_4 \beta_5(E, R) + 2\beta_6(E, R) - P_3 \beta_3(R)}{2(1+e^{R+\theta_2})(e^{2E} + 2e^{E-\theta_1} + 1)(1+e^{R-\theta_2}) + 2(1+e^{E+\theta_1})(1+e^{E-\theta_1})(2+e^{R+\theta_2} + e^{R-\theta_2})} + \frac{P_1 P_3 \beta_1(E, R)}{2(1+e^{E+\theta_1})(3+e^{R+\theta_2})} \right] HR + \left[\frac{(P_2 P_4 - P_1 P_3) \beta_1(E, R) + P_2 \beta_4(E, R) + 2P_4 \beta_5(E, R) + 2\beta_6(E, R) - P_1 \beta_2(E)}{2(1+e^{R+\theta_2})(e^{2E} + 2e^{E-\theta_1} + 1)(1+e^{R-\theta_2}) + 2(1+e^{E+\theta_1})(1+e^{E-\theta_1})(2+e^{R+\theta_2} + e^{R-\theta_2})} + \frac{P_1 P_3 \beta_1(E, R)}{2(1+e^{E+\theta_1})(3+e^{R+\theta_2})} \right] HE + \left[\frac{P_2 P_4 - P_1 P_3 + P_2 + P_4 - P_1 - P_3}{2(1+e^{R+\theta_2})(e^{2E} + 2e^{E-\theta_1} + 1)(1+e^{R-\theta_2}) + 2(1+e^{E+\theta_1})(1+e^{E-\theta_1})(2+e^{R+\theta_2} + e^{R-\theta_2})} + \frac{P_1 P_3 - 1}{2(1+e^{E+\theta_1})(3+e^{R+\theta_2})} \right] H. \tag{A13}$$

7. IC8

$$\begin{aligned}
\Delta u_{IC_8} = & \left[\frac{P_2 P_4 \beta_1(E, R)}{2(1 + e^{E-\theta_1})(1 + 3e^{R-\theta_2})} \right. \\
& + \left. \frac{(P_1 P_3 - P_2 P_4) \beta_1(E, R) + 2P_1 \beta_4(E, R) + P_3 \beta_5(E, R) + 2\beta_6(E, R) - P_4 \beta_3(R)}{2(1 + e^{-R+\theta_2})(e^{-R-\theta_2} + e^{-E+\theta_1} + 2)(1 + e^{E+\theta_1}) + 2(1 + e^{-E+\theta_1})(1 + e^{-R-\theta_2})(2 + e^{-R+\theta_2} + e^{E+\theta_1})} \right] HR \\
& + \left[\frac{P_2 P_4 \beta_1(E, R)}{2(1 + e^{E-\theta_1})(1 + 3e^{R-\theta_2})} \right. \\
& + \left. \frac{(P_1 P_3 - P_2 P_4) \beta_1(E, R) + P_1 \beta_4(E, R) + 2P_3 \beta_5(E, R) + 2\beta_6(E, R) - P_2 \beta_2(E)}{2(1 + e^{-R+\theta_2})(e^{-R-\theta_2} + e^{-E+\theta_1} + 2)(1 + e^{E+\theta_1}) + 2(1 + e^{-E+\theta_1})(1 + e^{-R-\theta_2})(2 + e^{-R+\theta_2} + e^{E+\theta_1})} \right] HE \\
& + \left[\frac{P_2 P_4 - 1}{2(1 + e^{E-\theta_1})(1 + 3e^{R-\theta_2})} \right. \\
& + \left. \frac{P_1 P_3 - P_2 P_4 + P_1 + P_3 - P_2 - P_4}{2(1 + e^{-R+\theta_2})(e^{-R-\theta_2} + e^{-E+\theta_1} + 2)(1 + e^{E+\theta_1}) + 2(1 + e^{-E+\theta_1})(1 + e^{-R-\theta_2})(2 + e^{-R+\theta_2} + e^{E+\theta_1})} \right] H.
\end{aligned} \tag{A14}$$

8. IC9

$$\begin{aligned}
\Delta u_{IC_9} = & \left[\frac{P_2 P_4 \beta_1(E, R) + P_4 \beta_5(E, R)}{2(e^{R-\theta_2} + e^{E+\theta_1} + 2)(1 + e^{E-\theta_1}) + 4e^{E-\theta_1}(1 + e^{R-\theta_2})(1 + e^{E+\theta_1})} + \frac{P_1 P_3 \beta_1(E, R) + P_3 \beta_5(E, R)}{2(2 + e^{R+\theta_2})(1 + e^{E-\theta_1})(1 + e^{E+\theta_1}) + 2e^{E-\theta_1}(1 + e^{R+\theta_2})(1 + e^{E+\theta_1})} \right] HR \\
& + \left[\frac{P_2 P_4 \beta_1(E, R) + 2P_4 \beta_5(E, R) - P_1 \beta_2(E)}{2(e^{R-\theta_2} + e^{E+\theta_1} + 2)(1 + e^{E-\theta_1}) + 4e^{E-\theta_1}(1 + e^{R-\theta_2})(1 + e^{E+\theta_1})} + \frac{P_1 P_3 \beta_1(E, R) + 2P_3 \beta_5(E, R) - P_2 \beta_2(E)}{2(2 + e^{R+\theta_2})(1 + e^{E-\theta_1})(1 + e^{E+\theta_1}) + 2e^{E-\theta_1}(1 + e^{R+\theta_2})(1 + e^{E+\theta_1})} \right] HE \\
& + \left[\frac{P_2 P_4 + P_4 - P_1 - 1}{2(e^{R-\theta_2} + e^{E+\theta_1} + 2)(1 + e^{E-\theta_1}) + 4e^{E-\theta_1}(1 + e^{R-\theta_2})(1 + e^{E+\theta_1})} + \frac{P_1 P_3 + P_3 - P_2 - 1}{2(2 + e^{R+\theta_2})(1 + e^{E-\theta_1})(1 + e^{E+\theta_1}) + 2e^{E-\theta_1}(1 + e^{R+\theta_2})(1 + e^{E+\theta_1})} \right] H.
\end{aligned} \tag{A15}$$

9. IC10

$$\begin{aligned}
\Delta u_{IC_{10}} = & \left[\frac{P_2 P_4 \beta_1(E, R) + P_4 \beta_5(E, R)}{2(2 + e^{E+\theta_1})(1 + e^{E-\theta_1})(1 + e^{R-\theta_2}) + 2e^{R-\theta_2}(1 + e^{E-\theta_1})(1 + e^{E+\theta_1})} \right. \\
& + \left. \frac{P_1 P_3 \beta_1(E, R) + P_3 \beta_5(E, R)}{2(1 + e^{R+\theta_2})(1 + e^{E-\theta_1})(3 + e^{E+\theta_1}) + 2e^{E-\theta_1}(1 + e^{R+\theta_2})(1 + e^{E+\theta_1})} \right] HR \\
& + \left[\frac{P_2 P_4 \beta_1(E, R) + 2P_4 \beta_5(E, R) - P_1 \beta_2(E)}{2(2 + e^{E+\theta_1})(1 + e^{E-\theta_1})(1 + e^{R-\theta_2}) + 2e^{R-\theta_2}(1 + e^{E-\theta_1})(1 + e^{E+\theta_1})} \right. \\
& + \left. \frac{P_1 P_3 \beta_1(E, R) + 2P_3 \beta_5(E, R) - P_2 \beta_2(E)}{2(1 + e^{R+\theta_2})(1 + e^{E-\theta_1})(3 + e^{E+\theta_1}) + 2e^{E-\theta_1}(1 + e^{R+\theta_2})(1 + e^{E+\theta_1})} \right] HE \\
& + \left[\frac{P_2 P_4 + P_4 - P_1 - 1}{2(2 + e^{E+\theta_1})(1 + e^{E-\theta_1})(1 + e^{R-\theta_2}) + 2e^{R-\theta_2}(1 + e^{E-\theta_1})(1 + e^{E+\theta_1})} \right. \\
& + \left. \frac{P_1 P_3 + P_3 - P_2 - 1}{2(1 + e^{R+\theta_2})(1 + e^{E-\theta_1})(3 + e^{E+\theta_1}) + 2e^{E-\theta_1}(1 + e^{R+\theta_2})(1 + e^{E+\theta_1})} \right] H.
\end{aligned} \tag{A16}$$

10. IC11

$$\begin{aligned} \Delta u_{IC_{11}} = & \left[\frac{P_2 P_4 \beta_1(E, R)}{2(1+3e^{E-\theta_1})(1+e^{R-\theta_2})} + \frac{(P_1 P_3 - P_2 P_4) \beta_1(E, R) + 2P_1 \beta_4(E, R) + P_3 \beta_5(E, R) + 2\beta_6(E, R) - P_4 \beta_3(R)}{2(1+e^{R+\theta_2})(2e^{2E} + e^{E-\theta_1} + e^{E+\theta_1})(1+e^{R-\theta_2}) + 2(1+e^{E+\theta_1})(1+e^{E-\theta_1})(1+2e^{R-\theta_2} + e^{2R})} \right] HR \\ & + \left[\frac{P_2 P_4 \beta_1(E, R)}{2(1+3e^{E-\theta_1})(1+e^{R-\theta_2})} + \frac{(P_1 P_3 - P_2 P_4) \beta_1(E, R) + P_1 \beta_4(E, R) + 2P_3 \beta_5(E, R) + 2\beta_6(E, R) - P_2 \beta_2(E)}{2(1+e^{R+\theta_2})(2e^{2E} + e^{E-\theta_1} + e^{E+\theta_1})(1+e^{R-\theta_2}) + 2(1+e^{E+\theta_1})(1+e^{E-\theta_1})(1+2e^{R-\theta_2} + e^{2R})} \right] HE \quad (A17) \\ & + \left[\frac{P_2 P_4 - 1}{2(1+3e^{E-\theta_1})(1+e^{R-\theta_2})} + \frac{P_1 P_3 - P_2 P_4 + P_1 + P_3 - P_2 - P_4}{2(1+e^{R+\theta_2})(2e^{2E} + e^{E-\theta_1} + e^{E+\theta_1})(1+e^{R-\theta_2}) + 2(1+e^{E+\theta_1})(1+e^{E-\theta_1})(1+2e^{R-\theta_2} + e^{2R})} \right] H. \end{aligned}$$

11. IC12

$$\begin{aligned} \Delta u_{IC_{12}} = & \left[\frac{(P_2 P_4 - P_1 P_3) \beta_1(E, R) + 2P_2 \beta_4(E, R) + P_4 \beta_5(E, R) + 2\beta_6(E, R) - P_3 \beta_3(R)}{2(1+e^{R+\theta_2})(2+e^{E+\theta_2} + e^{E-\theta_2})(1+e^{R-\theta_2}) + 2(1+e^{E+\theta_1})(1+e^{E-\theta_1})(e^{2R} + 2e^{R-\theta_1} + 1)} + \frac{P_1 P_3 \beta_1(E, R)}{2(3+e^{E+\theta_1})(1+e^{R+\theta_2})} \right] HR \\ & + \left[\frac{(P_2 P_4 - P_1 P_3) \beta_1(E, R) + P_2 \beta_4(E, R) + 2P_4 \beta_5(E, R) + 2\beta_6(E, R) - P_1 \beta_2(E)}{2(1+e^{R+\theta_2})(2+e^{E+\theta_2} + e^{E-\theta_2})(1+e^{R-\theta_2}) + 2(1+e^{E+\theta_1})(1+e^{E-\theta_1})(e^{2R} + 2e^{R-\theta_1} + 1)} + \frac{P_1 P_3 \beta_1(E, R)}{2(3+e^{E+\theta_1})(1+e^{R+\theta_2})} \right] HE \quad (A18) \\ & + \left[\frac{P_2 P_4 - P_1 P_3 + P_2 + P_4 - P_1 - P_3}{2(1+e^{R+\theta_2})(2+e^{E+\theta_2} + e^{E-\theta_2})(1+e^{R-\theta_2}) + 2(1+e^{E+\theta_1})(1+e^{E-\theta_1})(e^{2R} + 2e^{R-\theta_1} + 1)} + \frac{P_1 P_3 - 1}{2(3+e^{E+\theta_1})(1+e^{R+\theta_2})} \right] H. \end{aligned}$$

12. IC13

$$\begin{aligned} \Delta u_{IC_{13}} = & \left[\frac{(P_2 P_4 - P_1 P_3) \beta_1(E, R) + 2P_2 \beta_4(E, R) + P_4 \beta_5(E, R) + 2\beta_6(E, R) - P_3 \beta_3(R)}{2(1+e^{R+\theta_2})(e^{2E} + 2e^{E-\theta_1} + 1)(1+e^{R-\theta_2}) + 2(1+e^{E+\theta_1})(1+e^{E-\theta_1})(2+e^{R+\theta_2} + e^{R-\theta_2})} \right. \\ & \left. + \frac{P_1 P_3 \beta_1(E, R)}{2(3+e^{E+\theta_1})(1+e^{R+\theta_2})} \right] HR \\ & + \left[\frac{(P_2 P_4 - P_1 P_3) \beta_1(E, R) + P_2 \beta_4(E, R) + 2P_4 \beta_5(E, R) + 2\beta_6(E, R) - P_1 \beta_2(E)}{2(1+e^{R+\theta_2})(e^{2E} + 2e^{E-\theta_1} + 1)(1+e^{R-\theta_2}) + 2(1+e^{E+\theta_1})(1+e^{E-\theta_1})(2+e^{R+\theta_2} + e^{R-\theta_2})} \right. \\ & \left. + \frac{P_1 P_3 \beta_1(E, R)}{2(3+e^{E+\theta_1})(1+e^{R+\theta_2})} \right] HE \quad (A19) \\ & + \left[\frac{P_2 P_4 - P_1 P_3 + P_2 + P_4 - P_1 - P_3}{2(1+e^{R+\theta_2})(e^{2E} + 2e^{E-\theta_1} + 1)(1+e^{R-\theta_2}) + 2(1+e^{E+\theta_1})(1+e^{E-\theta_1})(2+e^{R+\theta_2} + e^{R-\theta_2})} \right. \\ & \left. + \frac{P_1 P_3 - 1}{2(3+e^{E+\theta_1})(1+e^{R+\theta_2})} \right] H. \end{aligned}$$

13. IC14

$$\begin{aligned}
\Delta u_{IC14} = & \left[\frac{P_2 P_4 \beta_1(E, R)}{2(1 + 3e^{E-\theta_1})(1 + e^{R-\theta_2})} \right. \\
& + \frac{(P_1 P_3 - P_2 P_4) \beta_1(E, R) + 2P_1 \beta_4(E, R) + P_3 \beta_5(E, R) + 2\beta_6(E, R) - P_4 \beta_3(R)}{2(1 + e^{-R+\theta_2})(e^{-R-\theta_2} + e^{-E+\theta_1} + 2)(1 + e^{E+\theta_1}) + 2(1 + e^{-E+\theta_1})(1 + e^{-R-\theta_2})(2 + e^{-R+\theta_2} + e^{E+\theta_1})} \Big] HR \\
& + \left[\frac{P_2 P_4 \beta_1(E, R)}{2(1 + 3e^{E-\theta_1})(1 + e^{R-\theta_2})} \right. \\
& + \frac{(P_1 P_3 - P_2 P_4) \beta_1(E, R) + P_1 \beta_4(E, R) + 2P_3 \beta_5(E, R) + 2\beta_6(E, R) - P_2 \beta_2(E)}{2(1 + e^{-R+\theta_2})(e^{-R-\theta_2} + e^{-E+\theta_1} + 2)(1 + e^{E+\theta_1}) + 2(1 + e^{-E+\theta_1})(1 + e^{-R-\theta_2})(2 + e^{-R+\theta_2} + e^{E+\theta_1})} \Big] HE \\
& + \left[\frac{P_2 P_4 - 1}{2(1 + 3e^{E-\theta_1})(1 + e^{R-\theta_2})} \right. \\
& + \left. \frac{P_1 P_3 - P_2 P_4 + P_1 + P_3 - P_2 - P_4}{2(1 + e^{-R+\theta_2})(e^{-R-\theta_2} + e^{-E+\theta_1} + 2)(1 + e^{E+\theta_1}) + 2(1 + e^{-E+\theta_1})(1 + e^{-R-\theta_2})(2 + e^{-R+\theta_2} + e^{E+\theta_1})} \right] H.
\end{aligned} \tag{A20}$$

14. IC15

$$\begin{aligned}
\Delta u_{IC15} = & \left[\frac{P_2 P_4 \beta_1(E, R) + P_4 \beta_5(E, R)}{2(e^{R-\theta_2} + e^{E+\theta_1} + 2)(1 + e^{E-\theta_1}) + 4e^{E-\theta_1}(1 + e^{R-\theta_2})(1 + e^{E+\theta_1})} \right. \\
& + \frac{P_1 P_3 \beta_1(E, R) + P_3 \beta_5(E, R)}{2(1 + e^{R+\theta_2})(1 + e^{E-\theta_1})(3 + e^{E+\theta_1}) + 2e^{E-\theta_1}(1 + e^{R+\theta_2})(1 + e^{E+\theta_1})} \Big] HR \\
& + \left[\frac{P_2 P_4 \beta_1(E, R) + 2P_4 \beta_5(E, R) - P_1 \beta_2(E)}{2(e^{R-\theta_2} + e^{E+\theta_1} + 2)(1 + e^{E-\theta_1}) + 4e^{E-\theta_1}(1 + e^{R-\theta_2})(1 + e^{E+\theta_1})} \right. \\
& + \frac{P_1 P_3 \beta_1(E, R) + 2P_3 \beta_5(E, R) - P_2 \beta_2(E)}{2(1 + e^{R+\theta_2})(1 + e^{E-\theta_1})(3 + e^{E+\theta_1}) + 2e^{E-\theta_1}(1 + e^{R+\theta_2})(1 + e^{E+\theta_1})} \Big] HE \\
& + \left[\frac{P_2 P_4 + P_4 - P_1 - 1}{2(e^{R-\theta_2} + e^{E+\theta_1} + 2)(1 + e^{E-\theta_1}) + 4e^{E-\theta_1}(1 + e^{R-\theta_2})(1 + e^{E+\theta_1})} \right. \\
& + \left. \frac{P_1 P_3 + P_3 - P_2 - 1}{2(1 + e^{R+\theta_2})(1 + e^{E-\theta_1})(3 + e^{E+\theta_1}) + 2e^{E-\theta_1}(1 + e^{R+\theta_2})(1 + e^{E+\theta_1})} \right] H.
\end{aligned} \tag{A21}$$